Phytoplankton consortia as a blueprint for mutually beneficial eukaryote-bacteria ecosystems: Biocoenosis of *Botryococcus* consortia

Olga Blifernez-Klassen[1,2*], Viktor Klassen[1,2], Daniel Wibberg[2], Enis Cebeci[1], Christian Henke[2,3], Christian Rückert[2], Swapnil Chaudhari[1,2], Oliver Rupp[4], Jochen Blom[4], Anika Winkler[2], Arwa Al-Dilaimi[2], Alexander Goesmann[4], Alexander Sczyrba[2,3], Jörn Kalinowski[2], Andrea Bräutigam[2,5], Olaf Kruse[1,2*]

[1]Algae Biotechnology and Bioenergy, Faculty of Biology, Bielefeld University, Universitätsstrasse 27, 33615 Bielefeld, Germany

[2]Center for Biotechnology (CeBiTec), Bielefeld University, Universitätsstrasse 27, 33615 Bielefeld, Germany

[3]Computational Metagenomics, Faculty of Technology, Bielefeld University, Universitätsstrasse 25, 33615 Bielefeld, Germany

[4]Bioinformatics and Systems Biology, Justus-Liebig-University, Heinrich-Buff-Ring 58, 35392 Gießen, Germany

[5]Computational Biology, Faculty of Biology, Bielefeld University, Universitätsstrasse 27, 33615 Bielefeld, Germany

*Address correspondence to: Olaf Kruse, olaf.kruse@uni-bielefeld.de or
Olga Blifernez-Klassen olga.blifernez@uni-bielefeld.de

Running title: Biocoenosis of *Botryococcus* consortia

Abstract

Bacteria occupy all major ecosystems and maintain an intensive relationship to the eukaryotes, developing together into complex biomes (i.e., phycosphere and rhizosphere). Interactions between eukaryotes and bacteria range from cooperative to competitive, with the associated microorganisms affecting their host`s development, growth, health and disease. Since the advent of non-culture dependent analytical techniques such as metagenome sequencing, consortia have been described but owing to the complex interactions rarely functionally dissected. Multifaceted analysis of the microbial consortium of the ancient phytoplankton *Botryococcus* as an attractive model food web revealed that its all abundant bacterial members belong to a distinct niche of biotin auxotrophs, essentially depending on the microalga. In addition, hydrocarbonoclastic bacteria without vitamin auxotrophies, which adversely affect the algal cell morphology, appear evidently decimated. Synthetic rearrangement of a minimal community consisting of alga, mutualistic and parasitic bacteria underpins the model of a eukaryote that domesticates its own mutualistic bacterial "zoo" to manipulate and control its surrounding biosphere. This model of domestication of mutualistic bacteria for the defense against destruents by a eukaryotic host could represent ecologically relevant interactions that cross species boundaries. Metabolic and system reconstruction disentangles the relationships and provide a blueprint for the construction of mutually beneficial synthetic ecosystems.

Keywords: eukaryote-bacteria interactions, phycosphere, mutualism, parasitism, microbiome, biotin (B-vitamin) auxotrophy, *Botryococcus braunii*, synthetic ecosystem, (meta)genome reconstruction

68 **Background**

69 Bacteria are omnipresent and affect likely every eukaryotic system through their presence
70 (Grosberg and Strathmann, 2007). Microalgae are the dominant primary producers and the
71 base of the food web within aquatic ecosystems and sustain in the natural environment in
72 close relationship with multiple associated microorganisms (Ramanan et al., 2016; Seymour
73 et al., 2017). Thus, the interactions between phytoplankton and bacteria represent a
74 fundamental ecological relationship within aquatic environments (Seymour et al., 2017), by
75 controlling nutrient cycling and biomass production at the food web base. The nature of the
76 exchange of micro- and macronutrients, diverse metabolites including complex products such
77 as polysaccharides, and infochemicals defines the relationship of the symbiotic partners (Cole,
78 1982; Amin et al., 2015; Zengler and Zaramela, 2018), which span mutualism, commensalism
79 and parasitism (Ramanan et al., 2016). Within a parasitic association, the bacteria are known
80 to adversely affect the algae (Wang et al., 2010), while in commensalism the partners can
81 survive independently, with the commensal feeding on algae-provided substrates, but without
82 harming the host (Ramanan et al., 2016). Mutualistic interactions include *i.a.* the obligate
83 relationships between vitamin-synthesizing bacteria and vitamin-auxotrophic phytoplankton
84 species (Croft et al., 2005). Many microalgae cannot synthesize several growth-essential
85 vitamins (like B_{12} and B_1) (Croft et al., 2005; Croft et al., 2006; Tang et al., 2010) and obtain
86 them through a symbiotic relationship with bacteria in exchange for organic carbon (Grant et
87 al., 2014). Recent observations suggest that not only certain microalgae require vitamins, but
88 many bacteria also have to compete with other organisms for the B-vitamins (Sañudo-
89 Wilhelmy et al., 2014; Gómez-Consarnau et al., 2018).

90 However, in microbial environments, where the distinction between host and symbionts is
91 less clear, the identification of the associated partners and the nature of their relationship is
92 challenging. Looking for a suitable model food web system to elucidate the complexity of
93 eukaryote-prokaryote interactions, we focused on the microalga-bacteria consortia with an
94 organic carbon-rich phycosphere. The planktonic chlorophyta *Botryococcus braunii* excretes
95 chemically inert long-chain hydrocarbons and a variety of exo-polysaccharides (Banerjee et
96 al., 2002) which allows this single celled alga to form large agglomerates (Grosberg and
97 Strathmann, 2007). Both organic carbon-based products are exposed to the surrounding
98 ecosystem and enable the alga to sustain in the natural environment (phycosphere) in close
99 relationship with multiple associated microorganisms (Ramanan et al., 2016; Seymour et al.,
100 2017). *Botryococcus* exudes up to 46% of their photosynthetically fixed carbon into the
101 phycosphere (Blifernez-Klassen et al., 2018), similarly to processes, however with lesser

102 extent, observed for seedlings as well as adult plants within the rhizosphere in the form of
103 poorly characterized rhizodeposits (Nguyen, 2003; Bisseling et al., 2009; Marschner, 2011).
104 *B. braunii* consortia, naturally accompanied with a variety of microorganisms (Chirac et al.,
105 1985), may represent an example for an association already existing during the early stages of
106 life development on earth, since it is generally considered that a progenitor of *Botryococcus*
107 impacted the development of today's oil reserves and coal shale deposits (McKirdy et al.,
108 1986). Thus, the microbiome associated with *Botryococcus braunii* presents a unique
109 opportunity to dissect the roles of the eukaryote and prokaryotes within the consortium and
110 test if and how the eukaryote manipulates its biome.

111 The interactions between *B. braunii* and the associated bacteria are not fully understood,
112 but are known to influence the microalgal growth performance and product formation
113 capacity (Chirac et al., 1985; Banerjee et al., 2002; Tanabe et al., 2015; Fuentes et al., 2016).
114 To understand the complex nature of the unique habitat of a microalgal phycosphere and to
115 unravel the food web between alga and bacteria, we investigated the consortia accompanying
116 the hydrocarbon/carbohydrate-producing green microalga *Botryococcus braunii*.
117

118 **Results and discussion**

119 **Metagenomic survey of the *Botryococcus braunii* consortia**

120 To determine the inhabitants of the *B. braunii* ecosystem, we profiled four different
121 *Botryococcus* communities (races A and B) using high-throughput 16S rDNA gene amplicon
122 and read-based metagenome sequencing approaches (Figures S1-3; Figure 1a). Assembly and
123 functional annotation of the metagenomes together with single strain isolation and sequencing
124 reconstructed the capabilities of the most abundant consortial microorganisms and were used
125 to design and test synthetic alga-bacteria ecosystems. The analysis of the 16S rDNA
126 amplicons and a read-based metagenome approach showed that each of the *B. braunii*
127 communities represents a comparable conserved consortium of a single algal and various
128 bacterial species as well as traces of Archaea and viruses (Figure S2). 16S rDNA amplicon
129 sequencing identified 33 bacterial taxa (Figure S3). The relative abundance of plastid 16S
130 rDNA sequences accounted up to 49 and 59% of all detected amplicon reads in race A and B
131 samples, respectively. Metagenomic assembly resulted in ten high quality draft genomes with
132 >80% assembled. Three additional genomes were closed by single strain sequencing (Figure
133 1; Tables S1 and S2; Supplementary Discussion, Chapter 1). The bacterial community varied
134 quantitatively, but not qualitatively between growth phases and strains (Figure S3). *B. braunii*
135 consortia are inhabited by the same bacterial phyla (*Proteobactreria*, *Bacteroidetes*,

Acidobacteria and *Actinobacteria*), albeit in different relative abundances, compared to those phyla which occupy the plant rhizosphere (Xu et al., 2018) and the mammals gut (Ley et al., 2008).

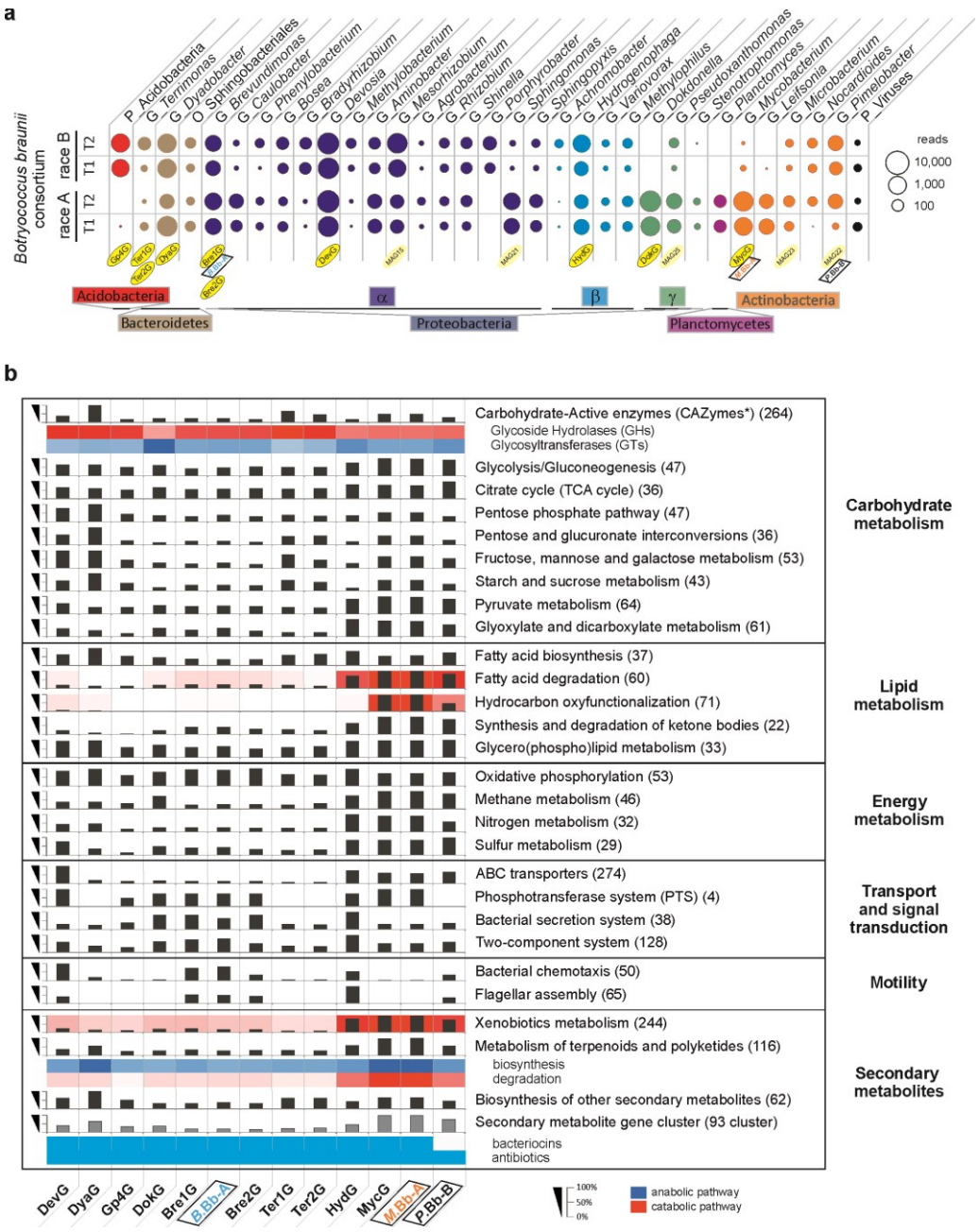

Figure 1: **Taxonomy of the *B. braunii* bacterial community and selected functional categories encoded in reconstructed MAGs and complete genomes.** (**a**) Normalized read-based comparison and taxonomic assignment of different *B. braunii* metagenome datasets. The circle size represents the amount of classified reads for the respective taxonomic group (minimum 50 reads per taxonomic group). (**b**) Abundance of selected functional categories encoded in the high-quality draft and complete bacterial genomes. Numbers in parentheses represent the maximal total number of genes within each pathway. Percentage: per cent of total number of genes per pathway identified within each genome. All annotated genes within the respective pathways are presented on the EMGB platform (https://emgb.cebitec.uni-bielefeld.de/Bbraunii-bacterial-consortium/). The pathways statistics are summarized in the Table S5.

150 During the growth phase, the *Botryococcus* phycosphere is dominated by the genera of
151 *Devosia*, *Dyadobacter*, *Dokdonella*, *Acidobacteria*, *Brevundimonas*, *Mesorhizobium* and
152 *Hydrogenophaga* which account for over 80% of the bacteria (Table S1). The re-processing
153 of the *B. braunii* Guadeloupe strain metagenome data (Sambles et al., 2017) and direct
154 comparison of the different datasets revealed the coinciding presence of the individual
155 bacterial genera, although massively varying in the abundance pattern in dependence of
156 cultivation conditions (Figure S5).The same taxa are also present *i.a.* in the active microbiome
157 associated roots and rhizosphere of oilseed rape (Gkarmiri et al., 2017), as well as in the
158 lettuce (Schreiter et al., 2014) and global citrus rhizosphere (Xu et al., 2018), strongly
159 suggesting an overall mutual dependence or preferred coexistence.
160 To identify genes that enable the bacterial community members to contribute to and to
161 benefit from the food web of the consortium, we performed a KEGG-based quantitative
162 functional assignment of the annotated high-quality MAGs (metagenome assembled
163 genomes). Based on these data sets, we sequenced genomes of isolated associates and
164 imported them to the EMGB platform (elastic metagenome browser, https://emgb.cebitec.uni-
165 bielefeld.de/Bbraunii-bacterial-consortium/; for details see Methods; Supplementary
166 Discussion, Chapter 2). We originally expected a uniform distribution of abilities and a high
167 degree of interconnectedness between all members of the consortium. Surprisingly, the
168 consortium divides into two functionally distinct groups of bacteria: The dominant consortia
169 members such as *Devosia* (DevG), *Dyadobacter* (DyaG) and *Brevundimonas* (Bre1G, *B.*Bb-
170 A) do not oxyfunctionalize hydrocarbons (Rojo, 2010), but their genomes are rich in genes
171 involved in the degradation/assimilation of carbohydrates (Figure 1b). On the contrary, the
172 bacterial strains *Mycobacterium* and *Pimelobacter* (*M.*Bb-A and *P.*Bb-B), which are of low
173 abundance within the consortia (Figure S3), contain a large portfolio of genes encoding
174 monooxygenases/hydroxylases for hydrocarbon degradation (Rojo, 2010) and hold the
175 potential for a pronounced catabolic capacity towards lipids, fatty acids and xenobiotics
176 (Figure 1b). Besides, *Mycobacterium* and *Pimelobacter* genomes were the only genomes
177 among the abundant community members to carry non-heme membrane-associated
178 monooxygenase *alkB* genes (Table S6). To test these observed genetic predisposition of the
179 consortia, we assessed algal capacities for growth and hydrocarbon production in co-
180 cultivation of the axenic *B. braunii* with one representative of each group.
181
182
183

184 **Effect of the bacterial community on the *B. braunii* host**

185 One representative of the core as well as less abundant community members were isolated
186 in axenic culture (*Brevundimonas* sp. Bb-A and *Mycobacterium* sp. Bb-A, respectively).
187 Synthetic algae-bacteria consortia were formed with an axenic hydrocarbon- and carbohydrate
188 producing *B. braunii* race A strain under strict phototrophic conditions (*e.g.* without the
189 supplementation of vitamins or organic carbon). Axenic *Botryococcus braunii* showed a
190 continuous increase in cell biomass and hydrocarbon content, yielding 2.1±0.2 gL^{-1} and
191 0.7±0.1 gL^{-1}, respectively (Figure 2a, b; Figure S6). Co-cultivation of the *Brevundimonas* sp.
192 Bb-A promotes growth of the alga and increases biomass by 60.5±16.9% compared to axenic
193 controls (Figure 2a) while co-cultivation with the *Mycobacterium* sp. Bb-A reduces growth by
194 30.6±4.8% (Figure 2b).
195

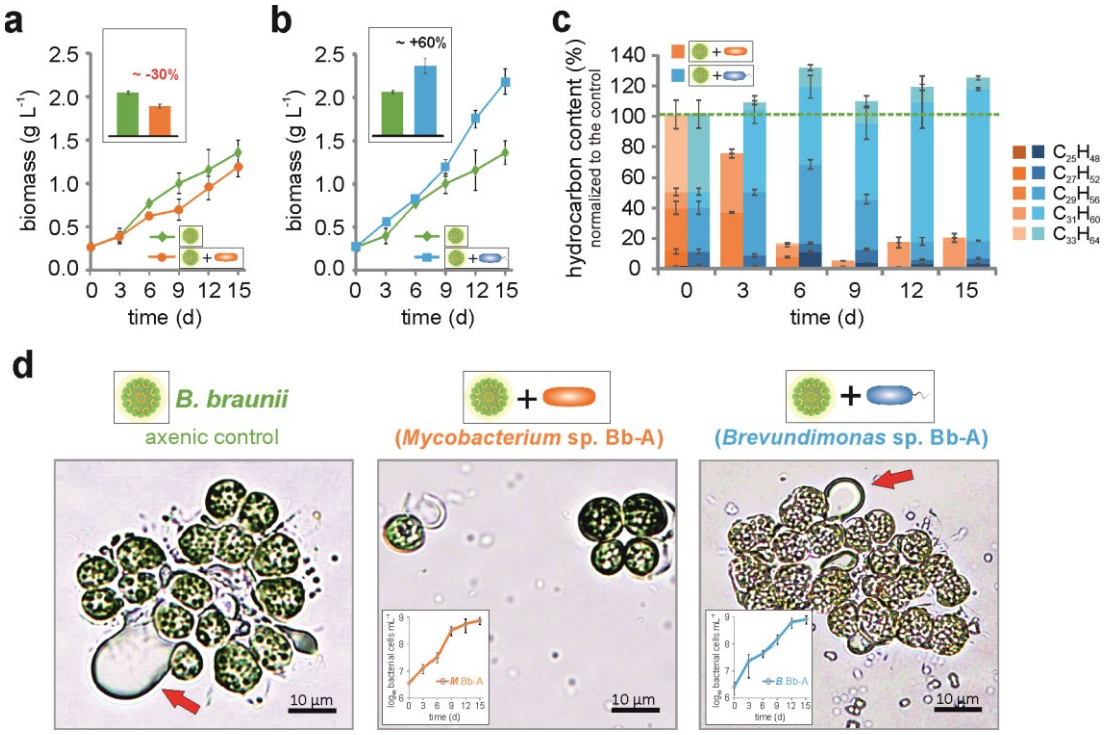

196

197 **Figure 2**: **Physiological effect of the individual bacterial isolates on the microalgae during co-**
198 **cultivation.** (**a-d**) Determination of algal growth and product formation performance of axenic and
199 xenic *B. braunii* cultures, supplemented with bacterial isolates. Shown are growth analysis of *B.*
200 *braunii* in the presence of (**a**) *Mycobacterium* sp. Bb-A and (**b**) *Brevundimonas* sp. Bb-A; (**c**)
201 comparison of the hydrocarbon levels observed in samples cultivated with bacterial isolates in relation
202 to the axenic *B. braunii* culture in the course of the cultivation; (**d**) morphological characteristic of
203 algal cells during the cultivation (9 days) with the bacterial isolates (red arrows indicate the
204 hydrocarbons produced by the microalga). Graphs imbedded in the pictures show the progress of the
205 bacterial growth (cell number on log_{10} scale).The error bars represent standard error of mean values of
206 three biological and three technical replicates (SE; n=9).
207

208 *B. braunii* accumulates hydrocarbons up to 38% of its dry weight (DW) in a bacteria-free
209 environment. In contrast, co-cultivation with *Mycobacterium* limits hydrocarbon
210 accumulation down to 4.4±0.2% of DW (Figure 2c) and alters colony morphology (Figure
211 2d). Loss of the hydrocarbon matrix reduces colony size (Figure 2d) and likely increases
212 susceptibility to grazers (Pančić and Kiørboe, 2018). The malfunction of colony formation
213 can thus be attributed to imbalanced and dysbiotic host-microbiome interaction similar to
214 imbalanced interactions previously observed (Gilbert et al., 2016; Durán et al., 2018) and
215 *Mycobacterium* essentially acts as a pathogen. The dramatic decrease in hydrocarbon content
216 and disturbed colony formation cannot be observed in cultures supplemented with
217 *Brevundimonas* or in the xenic *Botryococcus braunii* algae-bacteria communities (Figure 2c,
218 d; Figures S1 and S6), pointing to a balanced equilibrium between the alga and its
219 microbiome in natural environments.
220 Since *Botryococcus* readily releases huge amounts of organic carbon into the extracellular
221 milieu (Blifernez-Klassen et al., 2018), creating a phycosphere that naturally attracts many
222 microorganisms, including those with potential damaging effects, its evolutionary fitness will
223 depend on efficient management of the "bacterial zoo". We hypothesized that there is a strong
224 control mechanism that allows the algae host to attract and control symbiotic / beneficial
225 bacteria. Therefore, we examined the genetic portfolio of the bacterial community for
226 essential cofactors and interdependencies.
227
228 **The core community of *Botryococcus* phycosphere belongs to a distinct niche of biotin**
229 **auxotrophs**
230 At first glance, the *Botryococcus* alga does not appear to be obligatory dependent on a
231 bacterial community, since axenic strains can be fully photoautotrophically cultured without
232 vitamin supplements (Figure 2 a, b) and contains the vitamin B_{12}-independent form of
233 methionine synthase (*metE*) (Molnár et al., 2012). (Meta)Genome reconstruction revealed that
234 the *B. braunii* bacterial core community is auxotrophic for various B-vitamins (Figure 3a),
235 making them dependent on an exogenous supply of vitamins for survival. All abundant genera
236 within the *B. braunii* consortia (including the growth-promoting *Brevundimonas*) lack the
237 complete gene portfolio for biotin (vitamin B_7) synthesis (Figure 3a), but contained the
238 complete biosynthesis pathway of fatty acids for which biotin is essential (Sañudo-Wilhelmy
239 et al., 2014). The complete thiamin synthesis pathway (vitamin $B_{1,}$ essential for citrate cycle
240 and pentose phosphate pathway (Sañudo-Wilhelmy et al., 2014)) could not be reconstructed
241 for four assembled genomes. Five genera are auxotrophic for cobalamin (vitamin B_{12}).

242 Although, auxotrophic for various B-vitamins including biotin, the consortia's most abundant
243 species *Devosia* (DevG) contains the complete pathway for vitamin B_{12} synthesis. In view of
244 the fact that the bacterial abundance determines their functional relevance for the community
245 (Reed and Martiny, 2007; Rivett and Bell, 2018), this species is also likely to provide both the
246 bacterial community and the microalga with this vitamin (Croft et al., 2005), thus confirming
247 the recent proposition that the B_{12} supply is realized only by a few certain bacteria within the
248 alga-bacteria consortia (Krohn-Molt et al., 2017). In this context, since the B_7-auxotrophs are
249 prevalent within the detected consortia, it is doubtful that the large required supply of biotin is
250 of bacterial origin. Because of its predominance within the community (Figure S2), the
251 microalga is more likely to secrete and provide this vitamin to the bacteria.

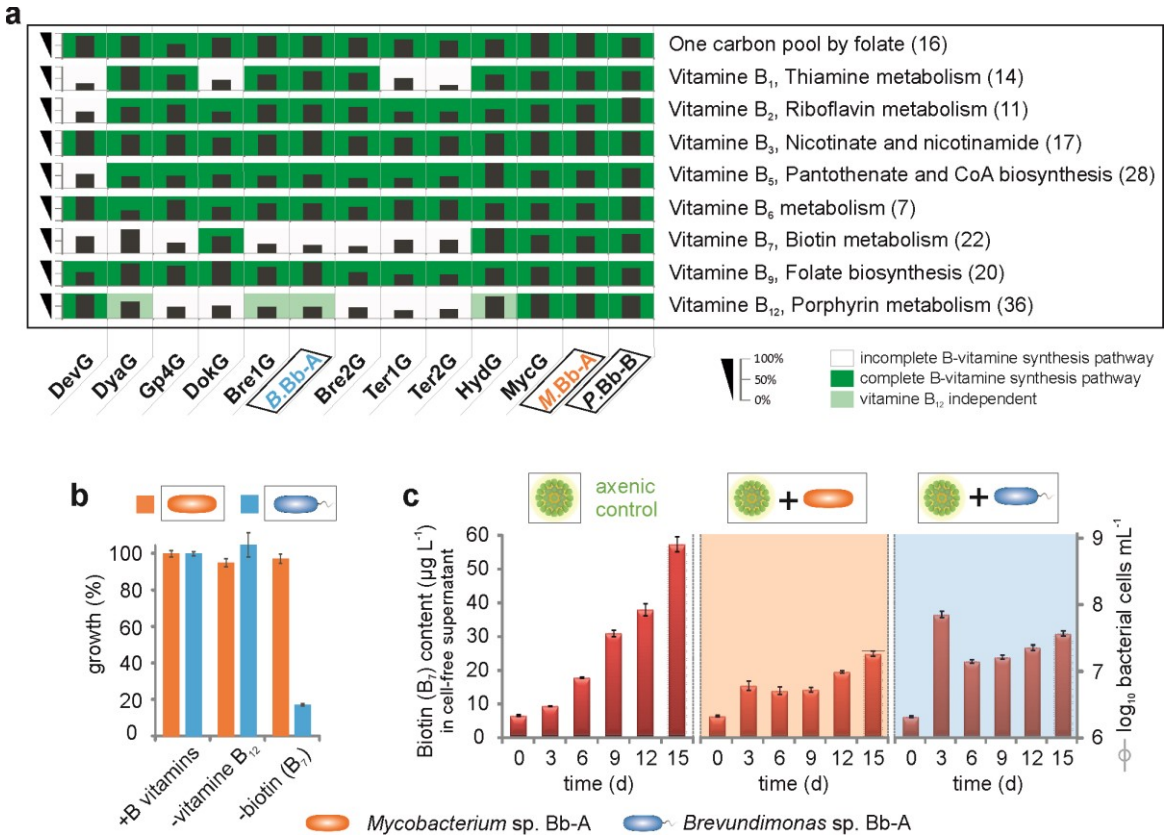

252

253 **Figure 3: Essential cofactors (inter-)dependencies of the bacterial core community and isolates**
254 **of *B. braunii*.** (**a**) Heatmap of the reconstructed *de novo* biosynthesis of B-vitamins encoded in the
255 high-quality draft and complete bacterial genomes. Numbers in parentheses represent the maximal
256 total number of genes within each pathway. Percentage: per cent of total number of genes per pathway
257 identified within each genome. All annotated genes within the respective pathways are presented on
258 the EMGB platform (https://emgb.cebitec.uni-bielefeld.de/Bbraunii-bacterial-consortium/). The
259 pathways statistics are summarized in the Table S5 and S8. (**b**) Growth assay to confirm B-vitamin
260 auxotrophy and prototrophy in axenic *Brevundimonas* sp. Bb-A (blue) and *Mycobacterium* sp. Bb-A
261 (orange) strains, respectively. (**c**) Biotin concentration levels detected in cell-free supernatants from
262 the cultures of axenic *B. braunii* as well as in the presence of *Mycobacterium* sp. Bb-A (orange) and
263 *Brevundimonas* sp. Bb-A (blue). The error bars represent standard error of mean values of three
264 biological and three technical replicates (SE; n=9).

265 It is well known, that many microalgae rely on the external supply of growth-essential
266 vitamins like cobalamin and thiamin (Croft et al., 2005; Croft et al., 2006; Tang et al., 2010),
267 however, biotin auxotrophy is rare among phytoplankton species (Croft et al., 2006). Here,
268 our genome reconstruction results strongly suggests that also bacteria have to compete with
269 other organisms for the B-vitamins and live in a close mutualistic relationship with the
270 microalga strongly depending on the biotin supply. The growth promoting effect of
271 *Brevundimonas* (Figure 2b), which depends on an exogenous supply of biotin for survival, is
272 thus based on the close interaction with the microalga. In contrast, low abundant consortial
273 members such as *Mycobacterium* are B-vitamin prototrophs (Figure 3a).
274 Extended experimental analysis confirmed the biotin (vitamin B_7) auxotrophy in
275 *Brevundimonas* sp. Bb-A and vitamin B prototrophy in *Mycobacterium* sp. Bb-A as deduced
276 from the assembled genomes (Figure 3b). *Botryococcus braunii* secrets biotin into the
277 surrounding environment (Figure 3c) and secretion is increasingly induced by the presence of
278 bacteria, particularly in the cultures with the B_7-auxotrophs (compare to Figure 3c at
279 timepoint 3 days). The secretion of some B-vitamins has already been observed in microalgae
280 (Aaronson et al., 1977), and also plants support their rhizosphere by active riboflavin (vitamin
281 B_2) excretion from their roots (Higa et al., 2008). However, the eukaryotic B-vitamin
282 secretion (especially of biotin), which was increasingly induced by the presence of bacteria, as
283 well as their simultaneous active uptake, remained so far unrecognized.
284 Collectively, in a healthy (natural) community, non-hydrocarbon degrading bacterial
285 genera which are auxotrophic for one or more vitamins dominate the phycosphere, while fully
286 prototrophic hydrocarbonoclastic bacteria are present but not abundant. We hypothesized that
287 *B. braunii* cultivates its own auxotrophic "bacterial zoo" to combat hydrocarbonoclastic
288 bacteria. To test the hypothesis, synthetic consortia of alga–"good bacteria"–"bad bacteria"
289 were formed and analyzed.
290
291 **Bacterial biotin-auxotrophic symbionts fend their eukaryotic host**
292 We hypothesized that the alga maintains its balanced, 'healthy' microbiome by recruiting
293 beneficial, vitamin B-auxotrophic microorganisms with the provision of photosynthetically
294 fixed carbon and biotin and thus counteracts pathogen assault. *Brevundimonas* and
295 *Mycobacterium* were co-cultivated with the axenic *Botryococcus* alga under photoautrophic
296 conditions with three different inoculum ratios (Figure 4a).
297
298

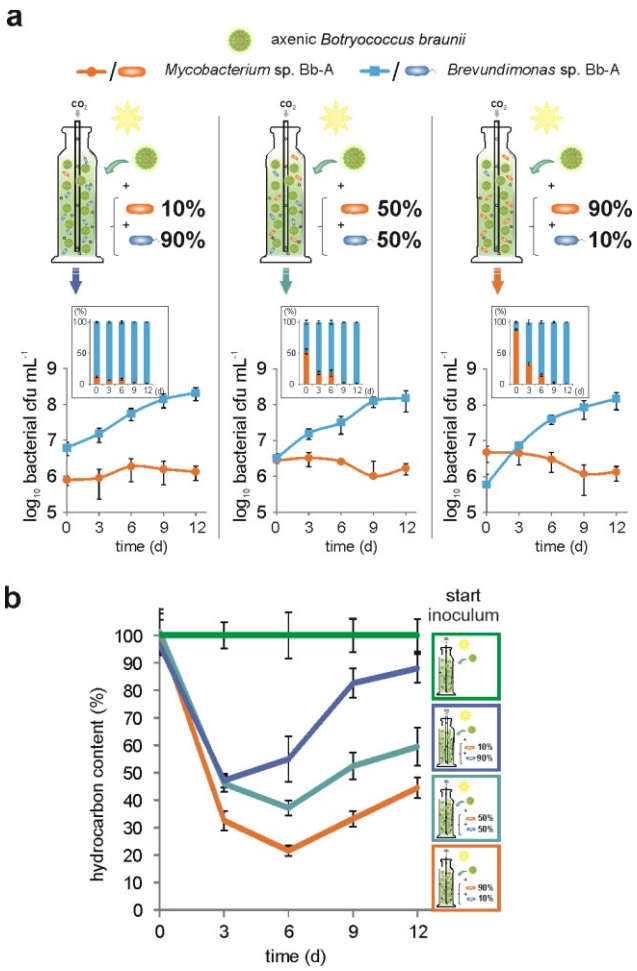

Figure 4: **Bacterial symbionts fend their eukaryotic host from hydrocarbonoclastic invaders.** Physiology of a synthetic alga-bacteria-bacteria community, consisting of *Brevundimonas* sp. Bb-A (blue) and *Mycobacterium* sp. Bb-A (orange) in co-culture with *B. braunii* (green) under photoautrophic conditions with three different inoculum ratios. Shown are (**a**) the progression of bacterial proliferation (cfu, colony-forming units) and (**b**) detected relative hydrocarbon levels (normalized to the axenic control) during the co-cultivation. The error bars represent standard error of mean values of three biological and three technical replicates (SE; n=9).

Independently from the initial amount of inoculum, biotin-auxotrophic *Brevundimonas* proliferated strongly within this synthetic community. *Mycobacterium* did not proliferate in the presence of *Brevundimonas* (Figure 4a), but was clearly capable of growth in the presence of the alga alone (Figure 2b). *Brevundimonas* apparently produces bioactive compounds with bacteriostatic properties, which likely decimate the proliferation of *Mycobacterium*. Indeed, all reconstructed genomes encode metabolic gene cluster for antibiotic compounds (especially against Gram-positive bacteria) and for bacteriocins (Figure 1b, Table S9) with significant antimicrobial potency (Cotter et al., 2013), the potential of which should be subject of further research. The protective effect of *Brevundimonas* is evident from the hydrocarbon content of cultures which increases with decreasing proportions of *Mycobacterium* (Figure 4b).

318 Experimental analyses (Figures 2-4) thus confirmed key conjectures derived from
319 metagenomic assemblies (Figure 1).

320 In conclusion, the interactions between the microalga and bacteria within the *Botryococcus*
321 *braunii* consortia depends on a complex interplay between all members, with the microalga as
322 the "conductor" in this play (Figure 5). Our observations indicate that the microalga is
323 associated with a "zoo" of largely supportive bacteria and suggest a framework in which the
324 microalga specifically attracts vitamin-auxotrophic bacterial species and domesticates them
325 by controlling vitamin supply. Since autark bacteria without vitamin auxotrophies are present
326 in small proportions only (Figure S3; Figure 3a), they are likely decimated by antibacterial
327 agents from the supportive community.

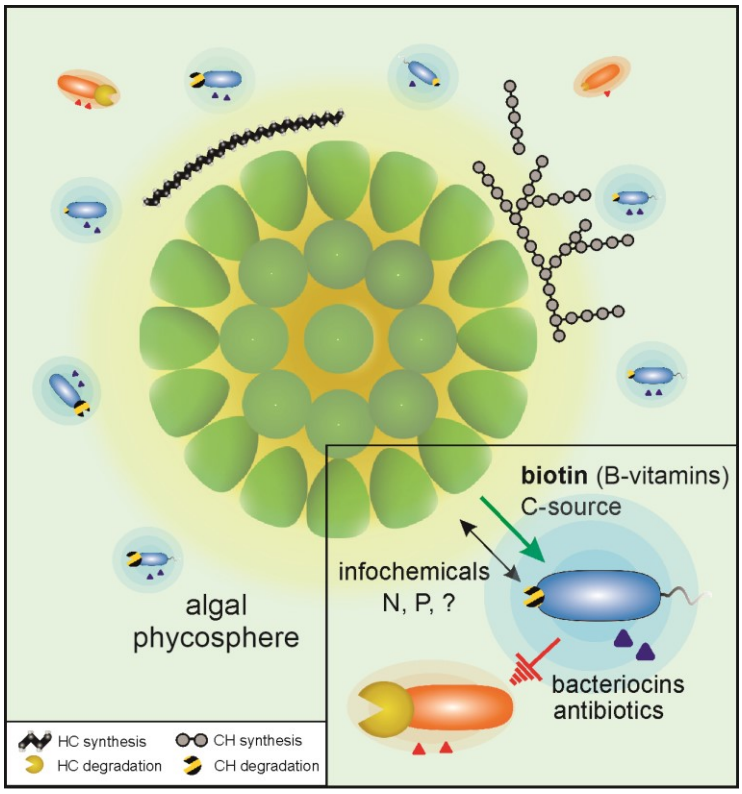

328

329 **Figure 5**: **Alga-bacteria interactions within the *Botryococcus braunii* phycosphere.** The depiction
330 summarizes the observed generic potential encoded in the (meta)genomes of bacterial associates
331 (Figures 1and 3), along with experimental validation within the minimal synthesis community
332 (Figures 2 and 4). The color code indicates the functional grouping of the community members:
333 supportive B-vitamin-auxotrophic (blue) and hydrocarbon-clastic prototrophic (red). The potential for
334 degradation of hydrocarbons and carbohydrates of the bacterial associates is illustrated via yellow and
335 striped pacmans, respectively. The genetic predisposition to the synthesis of bacteriocins and
336 antibiotics encoded by the secondary metabolite biosynthesis gene clusters, is indicated by the halos
337 and triangles, respectively. Abbreviation: HC, Hydrocarbons; CH, carbohydrates; B_7, Biotin; N,
338 nitrogen; P, phosphorus.
339

340 The analyses mechanistically resolved biotin as a critical metabolite and indicated the
341 presence of at least two additional communication signals: a bacterial signal increasing biotin

342 production (Figure 3c) and a bacteriostatic compound directed from *Brevundimonas* at
343 *Mycobacterium* (Figure 4a). The metagenomes hint at additional beneficial interactions
344 between the alga and its cultivated "zoo": vitamin B_{12}, and assimilated N and P from the
345 bacteria in exchange for biotin (and other vitamins) as well as carbon from the alga (Figure 5).
346 The successful design of minimal synthetic alga-bacteria cultures consisting only of two
347 bacteria species and the alga precisely demonstrates a functional triangle relationship for
348 preventing uncontrolled overgrowing of hydrocarbonoclastic destruents. However, the
349 elucidation of the communication signals exchanged between the participating parties will be
350 the subject of further research.
351 The metagenomic analysis of the *Botryococcus* consortium presents a path towards
352 mechanistic resolution of ecological interactions at the microscopic scale. Metabolic and
353 system reconstruction unravels the relations in the eukaryote-bacteria consortia and provides a
354 blueprint for the construction of mutually beneficial synthetic ecosystems.
355
356 **Methods**
357 **Strains, cultivation conditions and growth determination parameters.** Liquid, xenic
358 cultures of *Botryococcus braunii* race A (CCALA778, isolated in Serra da Estrela, Baragem
359 da Erva da Fome, Portugal) and race B (AC761, isolated from Paquemar, Martinique, France)
360 as well as the axenic *B. braunii* race A strain (SAG30.81, Peru, Dpto.Cuzco, Laguna Huaypo)
361 were used for co-cultivation studies. The cultures were phototrophically cultivated under 16:8
362 light-dark illumination of 350±400 μmol photons m^{-2} s^{-1} white light in modified Chu-13
363 media (without the addition of vitamin and organic carbon source) as described before
364 (Blifernez-Klassen et al., 2018). Carbon supply and agitation were achieved by bubbling the
365 cultures with moisture pre-saturated carbon dioxide-enriched air (5%, v/v) with a gas flow
366 rate of 0.05 vvm. Cultures growth was monitored by measurements of biomass organic dry
367 weight (DW) by drying 10 mL culture per sample (in three biological and technical replicates)
368 following the protocol described before (Astals et al., 2012). Additionally, microalgae and
369 bacteria cells were regularly checked by optical microscopy.
370 The bacterial isolates were obtained by plating highly diluted xenic *B. braunii* cultures
371 (CCALA778 and AC761) on LB agar plates supplied with vitamins (0.1 nM cobalamin, 3.26
372 nM thiamine and 0.1 nM biotin). After 1-2 weeks single cell colonies were picked, separately
373 plated and analyzed *via* 16S rDNA Sanger-sequencing by using the universal primer pair 27F
374 (5'-AGAGTTTGATCCTGGCTCAG-3') and 1385R (5'-CGGTGTGTRCAAGGCCC-3').
375 Two isolates, deriving from algal race A and one from race B, were classified based on full

376 length 16S rDNA similarity as *Mycobacterium* sp., *Brevundimonas* sp. and *Pimelobacter* sp.,
377 respectively. *Mycobacterium* sp. and *Brevundimonas* sp. were used for further analysis. The
378 purity of the axenic alga and bacterial strains was regularly verified by polymerase chain
379 reaction (PCR) amplification and Sanger-sequencing of the 16S rRNA gene using a universal
380 primer pair 27F and 1385R.
381 For experiments testing the requirement of B-vitamins, mono-cultures of *Mycobacterium* sp.
382 Bb-A and *Brevundimonas* sp. Bb-A were pre-washed three times in minimal medium
383 (Schlegel et al., 1961) and then starved of vitamins for two days prior to the start of the
384 experiment. Then, bacterial cells were diluted to 0.2 (oD_{600}) with minimal medium
385 supplemented with $1gL^{-1}$ glucose and B-vitamins (at the following concentrations: 0.1 nM
386 (each) of cobalamin, riboflavin, biotin and pantothenate as well as 3.26 nM thiamine) and
387 grown for seven days.
388 For the co-cultivation experiments, 500 mL axenic algal cultures (~0.25g L^{-1}) were inoculated
389 with the isolates (*Mycobacterium* sp. Bb-A or *Brevundimonas* sp. Bb-A, with ~$2x10^6$ cell mL^{-}
390 ^{1} for single isolate cultivation and with ~$2x10^6$ – $2x10^7$ cell mL^{-1} for co-cultivation with both
391 bacterial strains) and cultured under photoautotrophic conditions. The bacterial cell density
392 was determined by manual cell counting using hemocytometer or by determination of the
393 colony-forming units (cfu) as a proxy for viable population density using the replica plating
394 method (Jett et al., 1997).
395 The quantitative determination of the vitamin B_7 (biotin) concentration in cell-free
396 supernatants of the co-cultures and the axenic control was accomplished by using
397 microbiological microtiter plate test (VitaFast, r-biopharm, Darmstadt, Germany) according to
398 manufacturer instructions.
399 **Hydrocarbon extraction and analysis.** Hydrocarbon extraction was performed according to
400 the protocol published previously (Blifernez-Klassen et al., 2018). The dry extracted
401 hydrocarbons were resuspended in 500 µL of *n*-hexane, containing an internal standard *n*-
402 hexatriacontane ($C_{36}H_{74}$) and analysed *via* GC-MS and GC-FID as described before
403 (Schwarzhans et al., 2014; Blifernez-Klassen et al., 2018).
404 **DNA sample collection and preparation.** The samples from xenic *B. braunii* race A and B
405 cultures (three biological replicates) were taken in the linear and stationary growth phases
406 (after 9 and 24 days). Total community genomic DNA was extracted as previously described
407 (Zhou et al., 1996). The quality of the DNA was assessed by gel electrophoresis and the
408 quantity was estimated using the Quant-iT PicoGreen dsDNA Assay Kit (Invitrogen) and a
409 Tecan Infinite 200 Microplate Reader (Tecan Deutschland GmbH).

410 **High-throughput 16S rDNA amplicon sequencing.** To get insight into the community
411 composition of *B. braunii* Race A and B, high-throughput 16S rDNA amplicon sequencing
412 was performed as described recently by Maus et al (Maus et al., 2017). The primer pair
413 Pro341F (5′-CCTACGGGGNBGCASCAG-3′) and Pro805R (5′-
414 GACTACNVGGGTATCTAATCC-3′) was used to amplify the hypervariable regions V3 and
415 V4 of diverse bacterial and archaeal 16S rRNAs (Takahashi et al., 2014). In addition, the
416 primers also cover the 16S rDNA gene of algal chloroplasts and eukaryotic mitochondrial
417 genomes. Furthermore, in a two PCR steps based approach, multiplex identifier (MID) tags
418 and Illumina-specific sequencing adaptors were added to each amplicon. Only amplicons
419 featuring a size of ~460 bp were purified using AMPureXP® magnetic beads (Beckman
420 Coulter GmbH, Brea, California, USA). Resulting amplicons were qualitatively and
421 quantitatively analyzed using the Agilent 2100 Bioanalyzer system (Agilent Inc., Santa Clara,
422 California, USA) and pooled in equimolar amounts for paired-end sequencing on the Illumina
423 MiSeq system (Illumina, San Diego, California USA). This sequencing approach provided
424 ~150,000 reads per sample. An in-house pipeline as described previously (Wibberg et al.,
425 2016) was used for adapter and primer trimming of all samples. For amplicon processing, a
426 further in house amplicon processing pipeline including FLASH (Magoč and Salzberg, 2011),
427 USEARCH (Edgar, 2010) (v8.1), UPARSE (Edgar, 2013) and the RDP (Wang et al., 2007)
428 classifier (v2.9) was applied as described recently (Liebe et al., 2016; Klassen et al., 2017). In
429 summary, unmerged sequences resulting by FLASH (Magoč and Salzberg, 2011) (default
430 settings +-M 300) were directly filtered out. Furthermore, sequences with >1Ns (ambiguous
431 bases) and expected errors >0.5 were also discarded. Resulting data was further processed and
432 operational taxonomic units (OTUs) were clustered by applying USEARCH (Edgar, 2010)
433 (v8.1). The resulting OTUs were taxonomically classified using the RDP (Wang et al., 2007)
434 classifier (v2.9) in 16S modus (Threshold >0.8) and compared to the nt database by means of
435 BLASTN (O'Leary et al., 2016). In the last step, raw sequence reads were mapped back onto
436 the OTU sequences in order to get quantitative assignments.
437 **(Meta)Genome sequencing, assembly, binning and annotation.** For each of the four
438 samples (*B. braunii* race A and B from linear (T1) and stationary (T2) growth phase), the
439 genomic DNA from three replicates was pooled. To obtain the metagenome sequence, four
440 whole-genome-shotgun PCR-free sequencing libraries (Nextera DNA Sample Prep Kit;
441 Illumina, Munich, Germany) were generated based on the manufacturer's protocol
442 representing different time points of the cultivation and different algae communities. The four
443 libraries were sequenced in paired-end mode in a MiSeq run (2 x 300 bp) resulting in

444 11,963,558 and 11,567,552 reads for race A T1 and T2; 6,939,996 and 12,031,204 reads for
445 race B T1 and T2, respectively (total 12.75 Gb). The *de novo* metagenome assembly was
446 performed using the Ray Meta assembler (Boisvert et al., 2012) (v2.3.2) using a k-mer size of
447 41 and default settings. For contigs with length larger than 1 kb (n=127,914), the total
448 assembly size was 338.5 Mb, the N50=2,884 and the largest contig 1.59 Mb. All processed
449 raw sequence reads of the four samples were aligned to the assembled metagenome contigs by
450 means of Bowtie 2 (Langmead and Salzberg, 2012) (v2.2.4). By using SAMtools (Li et al.,
451 2009) (v1.6), the SAM files were converted to BAM files. These files were sorted and read
452 mapping statistics were calculated. The following portions of reads could be assembled to the
453 draft metagenomes: 70.1% and 77.5% for race A (T1 and T2); 51.0% and 62.9% for race B
454 (T1 and T2). For binning of the metagenome assembled genomes (MAGs), the tool MetaBAT
455 (v0.21.3) (Kang et al., 2015) was used with default settings. Completeness and contamination
456 of the resulting MAGs were tested with BUSCO (Simão et al., 2015; Waterhouse et al., 2018)
457 (v3.0.), using the Bacteria and Metazoa data set (Table S1).
458 For sequencing of the isolated species, 4 µg of purified chromosomal DNA was used to
459 construct PCR-free sequencing library and sequenced applying the paired protocol on an
460 Illumina MiSeq system, yielding ~1.71 Mio Reads (517 Mb in 3 Scaffolds, 58 Contigs) for
461 *Mycobacterium* sp. Bb-A and ~1.70 Mio Reads (503 Mb in 6 Scaffolds, 65 Contigs) for
462 *Pimelobacter* sp. Bb-B. Obtained sequences were *de novo* assembled using the GS *de novo*
463 Assembler software (v2.8, Roche). An *in silico* gap closure approach was performed as
464 described previously (Wibberg et al., 2011). MinION sequencing library with genomic DNA
465 from *Brevundimonas* sp. Bb-A was prepared using the Nanopore Rapid DNA Sequencing kit
466 (SQK-RAD04) according to the manufacturer's instructions with the following changes: The
467 entry DNA amount was increased to 800 ng and an AMPure XP bead cleanup was carried out
468 after transposon fragmentation. Sequencing was performed on an Oxford Nanopore MinION
469 Mk1b sequencer using a R9.5 flow cell, which was prepared according to the manufacturer's
470 instructions. MinKNOW (v1.13.1) was used to control the run using the 48h sequencing run
471 protocol; base calling was performed offline using albacore (v2.3.1). The assembly was
472 performed using canu v1.7 (Koren et al., 2017), resulting in a single, circular contig (170 Mb,
473 1kb to 17.5kb). This contig was then polished with Illumina short read data from the
474 metagenome data set using pilon (Walker et al., 2014), run for sixteen iterative cycles. bwa-
475 mem (Li and Wren, 2014) was used for read mapping in the first eight iterations and bowtie2
476 v2.3.2 (Langmead and Salzberg, 2012) in the second set of eight iterations. Annotation of the

477 draft chromosomes was performed within the PROKKA (Seemann, 2014) (v1.11) pipeline
478 and visualized using the GenDB 2.0 system (Meyer et al., 2003).
479 **Gene prediction, taxonomic assignment and functional characterization.** Gene prediction
480 on the assembled contigs of the MAGs was performed with Prodigal (Hyatt et al., 2010)
481 (v2.6.1) using the metagenome mode ("-p meta"). All genes were annotated and analyzed
482 with the in-house EMGB annotation system using the databases NCBI NR (O'Leary et al.,
483 2016), Pfam (Finn et al., 2014) and KEGG (Kanehisa et al., 2017). Based on DIAMOND
484 (Buchfink et al., 2015) (v0.8.36) hits against the NCBI-NR (O'Leary et al., 2016) database, all
485 genes were subject to taxonomic assignment using MEGAN (Huson et al., 2016).
486 Relationships to metabolic pathways were assigned based on DIAMOND (Buchfink et al.,
487 2015) hits against KEGG (Kanehisa et al., 2017). For Pfam (Finn et al., 2014) annotations,
488 pfamscan was used with default parameters. The genomes were manually inspected using an
489 E-value cutoff of $1x10^{-10}$ for several specific sequences listed Additional file 2, Table S6. The
490 profiling of the carbohydrate-active enzymes (CAZy) encoded by the *B. braunii* community
491 members was accomplished using dbCAN2 (Zhang et al., 2018) metaserver (Table S7). The
492 identification, annotation and analysis of the secondary metabolite biosynthesis gene clusters
493 within the MAGs and complete genomes were accomplished *via* the antiSMASH (Blin et al.,
494 2017) (v4.0) web server with default settings (Table S9).
495 **Phylogenetic analyses.** To assign and phylogenetically classify the MAGs, a core genome
496 tree was created by applying EDGAR (Blom et al., 2016) (v2.0). For calculation of a core-
497 genome-based phylogenetic tree, the core genes of all MAGs and the three isolates
498 *Mycobacterium* sp. Bb-A, *Brevundimonas* sp. Bb-A and *Pimelobacter* sp. Bb-B,
499 corresponding to selected reference sequences were considered. The implemented version of
500 FASTtree (Price et al., 2010) (using default settings) in EDGAR (Blom et al., 2016) (v2.0)
501 was used to create a phylogenetic Maximum-Likelihood tree based on 53 core genes (see
502 Table S4) of all genomes. Additionally, the MAGs were taxonomically classified on species
503 level by calculation of average nucleic and amino acid identities (ANI, AAI) by applying
504 EDGAR (Blom et al., 2016) (v2.0). For phylogenetic analysis of the 16S rDNA amplicon
505 sequences, MEGA (Kumar et al., 2016) (v7.0.26) was used. Phylogenetic tree was
506 constructed by means of Maximum-Likelihood Tree algorithm using Tamura 3-parameter
507 model. The robustness of the inferred trees was evaluated by bootstrap (1000 replications).
508 **Availability of data and materials**
509 The high-throughput 16S rDNA amplicon sequencing datasets obtained during the present
510 work are available at the EMBL-EBI database under BioProjectID PRJEB21978. The

511 metagenome datasets of *Botryococcus braunii* consortia as well as the resulting MAGs have
512 been deposited under the BioProjectIDs PRJEB26344 and PRJEB26345, respectively. The
513 genomes of the isolates *Brevundimonas* sp. Bb-A, *Mycobacterium* sp. BbA or *Pimelobacter*
514 sp. Bb-B are accessible under BioProjectIDs PRJNA528993, PRJEB28031 und PRJEB28032,
515 respectively. The communities most abundant ten high-quality draft as well as isolate
516 genomes are also accessible via EMGB platform (https://emgb.cebitec.uni-
517 bielefeld.de/Bbraunii-bacterial-consortium/).
518

519 **Authors' contributions**

520 O.B.K., V.K, and O.K. conceived this study. O.B.K., A.S., A.B., J.K. and O.K. supervised
521 experiments and analyses. O.B.K., V.K., E.C. and S.C. accomplished all physiological
522 studies. O.B.K., D.W., A.S., C.H., C.R., A.B., V.K., A.A.D., A.W., J.K., O.R., J.B. and A.G.
523 performed the sequencing and the bioinformatic analyses. O.B.K., V.K., A.B. and O.K. wrote
524 the original draft manuscript with contributions from all authors. O.B.K., V.K., A.B and O.K.
525 reviewed and edited the manuscript. All authors read and approved the final manuscript.
526

527 **Acknowledgements**

528 We are thankful to Joao Gouveia and Douwe van der Veen (Wageningen University, The
529 Netherlands) for providing *Botryococcus braunii* race A and B (CCALA778 and AC761)
530 stock cultures. Furthermore, we are grateful to the Center for Biotechnology (CeBiTec) at
531 Bielefeld University for access to the Technology Platforms.
532

533 **Funding**

534 This work was supported by the European Union Seventh Framework Programme (FP7/2007-
535 2013) under grant agreement 311956 (relating to project "SPLASH – Sustainable PoLymers
536 from Algae Sugars and Hydrocarbons"). The bioinformatics support by the BMBF-funded
537 project "Bielefeld-Gießen Center for Microbial Bioinformatics" – BiGi (grant 031A533)
538 within the German Network for Bioinformatics Infrastructure (de. NBI) is gratefully
539 acknowledged.
540

541 **Ethics approval and consent to participate**

542 Not applicable.
543

544 **Competing interests**

545 The authors declare that they have no competing interests

546

547 **References**

548 **Aaronson, S., Dhawale, S. W., Patni, N. J., Deangelis, B., Frank, O., and Baker, H.**
549 (1977). The cell content and secretion of water-soluble vitamins by several freshwater
550 algae. *Arch. Microbiol.* **112**:57–59.

551 **Amin, S. A., Hmelo, L. R., Van Tol, H. M., Durham, B. P., Carlson, L. T., Heal, K. R.,**
552 **Morales, R. L., Berthiaume, C. T., Parker, M. S., Djunaedi, B., et al.** (2015).
553 Interaction and signalling between a cosmopolitan phytoplankton and associated
554 bacteria. *Nature* **522**:98–101.

555 **Astals, S., Nolla-Ardèvol, V., and Mata-Alvarez, J.** (2012). Anaerobic co-digestion of pig
556 manure and crude glycerol at mesophilic conditions: Biogas and digestate. *Bioresour.*
557 *Technol.* **110**:63–70.

558 **Banerjee, A., Sharma, R., Chisti, Y., and Banerjee, U. C.** (2002). Botryococcus braunii: A
559 renewable source of hydrocarbons and other chemicals. *Crit. Rev. Biotechnol.* **22**:245–
560 279.

561 **Bisseling, T., Dangl, J. L., and Schulze-Lefert, P.** (2009). Next-Generation Communication.
562 *Science (80-.).* **324**:691 LP – 691.

563 **Blifernez-Klassen, O., Chaudhari, S., Klassen, V., Wördenweber, R., Steffens, T.,**
564 **Cholewa, D., Niehaus, K., Kalinowski, J., and Kruse, O.** (2018). Metabolic survey of
565 Botryococcus braunii: Impact of the physiological state on product formation. *PLoS One*
566 **13**:e0198976.

567 **Blin, K., Wolf, T., Chevrette, M. G., Lu, X., Schwalen, C. J., Kautsar, S. A.,**
568 **Suarez Duran, H. G., de los Santos, E. L. C., Kim, H. U., Nave, M., et al.** (2017).
569 antiSMASH 4.0—improvements in chemistry prediction and gene cluster boundary
570 identification. *Nucleic Acids Res.* **45**:W36–W41.

571 **Blom, J., Kreis, J., Spänig, S., Juhre, T., Bertelli, C., Ernst, C., and Goesmann, A.**
572 (2016). EDGAR 2.0: an enhanced software platform for comparative gene content
573 analyses. *Nucleic Acids Res.* **44**:W22–W28.

574 **Boisvert, S., Raymond, F., Godzaridis, E., Laviolette, F., and Corbeil, J.** (2012). Ray
575 Meta: scalable de novo metagenome assembly and profiling. *Genome Biol.* **13**:R122.

576 **Buchfink, B., Xie, C., and Huson, D. H.** (2015). Fast and sensitive protein alignment using
577 DIAMOND. *Nat. Methods* **12**:59–60.

578 **Chirac, C., Casadevall, E., Largeau, C., and Metzger, P.** (1985). Bacterial Influence Upon

579 Growth and Hydrocarbon Production of the Green Alga Botryococcus Braunii. *J.*
580 *Phycol.* **21**:380–387.
581 **Cole, J. J.** (1982). Interactions Between Bacteria and Algae in Aquatic Ecosystems. *Annu.*
582 *Rev. Ecol. Syst.* **13**:291–314.
583 **Cotter, P. D., Ross, R. P., and Hill, C.** (2013). Bacteriocins-a viable alternative to
584 antibiotics? *Nat. Rev. Microbiol.* **11**:95–105.
585 **Croft, M. T., Lawrence, A. D., Raux-Deery, E., Warren, M. J., and Smith, A. G.** (2005).
586 Algae acquire vitamin B12 through a symbiotic relationship with bacteria. *Nature*
587 **438**:90–93.
588 **Croft, M. T., Warren, M. J., and Smith, A. G.** (2006). Algae need their vitamins. *Eukaryot.*
589 *Cell* **5**:1175–1183.
590 **Durán, P., Thiergart, T., Garrido-Oter, R., Agler, M., Kemen, E., Schulze-Lefert, P.,**
591 **and Hacquard, S.** (2018). Microbial Interkingdom Interactions in Roots Promote
592 Arabidopsis Survival. *Cell* Advance Access published 2018,
593 doi:10.1016/j.cell.2018.10.020.
594 **Edgar, R. C.** (2010). Search and clustering orders of magnitude faster than BLAST.
595 *Bioinformatics* **26**:2460–2461.
596 **Edgar, R. C.** (2013). UPARSE: highly accurate OTU sequences from microbial amplicon
597 reads. *Nat. Methods* **10**:996–8.
598 **Finn, R. D., Bateman, A., Clements, J., Coggill, P., Eberhardt, R. Y., Eddy, S. R., Heger,**
599 **A., Hetherington, K., Holm, L., Mistry, J., et al.** (2014). Pfam: The protein families
600 database. *Nucleic Acids Res.* **42**.
601 **Fuentes, J. L., Garbayo, I., Cuaresma, M., Montero, Z., González-Del-Valle, M., and**
602 **Vílchez, C.** (2016). Impact of microalgae-bacteria interactions on the production of algal
603 biomass and associated compounds. *Mar. Drugs* **14**.
604 **Gilbert, J. A., Quinn, R. A., Debelius, J., Xu, Z. Z., Morton, J., Garg, N., Jansson, J. K.,**
605 **Dorrestein, P. C., and Knight, R.** (2016). Microbiome-wide association studies link
606 dynamic microbial consortia to disease. *Nature* **535**:94.
607 **Gkarmiri, K., Mahmood, S., Ekblad, A., Alström, S., Högberg, N., and Finlay, R.** (2017).
608 Identifying the Active Microbiome Associated with Roots and Rhizosphere Soil of
609 Oilseed Rape. *Appl. Environ. Microbiol.* **83**:e01938-17.
610 **Gómez-Consarnau, L., Sachdeva, R., Gifford, S. M., Cutter, L. S., Fuhrman, J. A.,**
611 **Sañudo-Wilhelmy, S. A., and Moran, M. A.** (2018). Mosaic patterns of B-vitamin
612 synthesis and utilization in a natural marine microbial community. *Environ. Microbiol.*

613 **20**:2809–2823.
614 **Grant, M. A. A., Kazamia, E., Cicuta, P., and Smith, A. G.** (2014). Direct exchange of
615 vitamin B12 is demonstrated by modelling the growth dynamics of
616 algal–bacterial cocultures. *ISME J.* **8**:1418–1427.
617 **Grosberg, R. K., and Strathmann, R. R.** (2007). The Evolution of Multicellularity: A
618 Minor Major Transition? *Annu. Rev. Ecol. Evol. Syst.* Advance Access published 2007,
619 doi:10.1146/annurev.ecolsys.36.102403.114735.
620 **Higa, A., Miyamoto, E., Rahman, L. ur, and Kitamura, Y.** (2008). Root tip-dependent,
621 active riboflavin secretion by Hyoscyamus albus hairy roots under iron deficiency. *Plant*
622 *Physiol. Biochem.* Advance Access published 2008, doi:10.1016/j.plaphy.2008.01.004.
623 **Huson, D. H., Beier, S., Flade, I., Górska, A., El-Hadidi, M., Mitra, S., Ruscheweyh, H.**
624 **J., and Tappu, R.** (2016). MEGAN Community Edition - Interactive Exploration and
625 Analysis of Large-Scale Microbiome Sequencing Data. *PLoS Comput. Biol.* **12**.
626 **Hyatt, D., Chen, G. L., LoCascio, P. F., Land, M. L., Larimer, F. W., and Hauser, L. J.**
627 (2010). Prodigal: Prokaryotic gene recognition and translation initiation site
628 identification. *BMC Bioinformatics* **11**.
629 **Jett, B. D., Hatter, K. L., Huycke, M. M., and Gilmore, M. S.** (1997). Simplified Agar
630 Plate Method for Quantifying Viable Bacteria. *Biotechniques* **23**:648–650.
631 **Kanehisa, M., Furumichi, M., Tanabe, M., Sato, Y., and Morishima, K.** (2017). KEGG:
632 New perspectives on genomes, pathways, diseases and drugs. *Nucleic Acids Res.*
633 **45**:D353–D361.
634 **Kang, D. D., Froula, J., Egan, R., and Wang, Z.** (2015). MetaBAT, an efficient tool for
635 accurately reconstructing single genomes from complex microbial communities. *PeerJ*
636 **3**:e1165.
637 **Klassen, V., Blifernez-Klassen, O., Wibberg, D., Winkler, A., Kalinowski, J., Posten, C.,**
638 **and Kruse, O.** (2017). Highly efficient methane generation from untreated microalgae
639 biomass. *Biotechnol. Biofuels* **10**:186.
640 **Koren, S., Walenz, B. P., Berlin, K., Miller, J. R., Bergman, N. H., and Phillippy, A. M.**
641 (2017). Canu: Scalable and accurate long-read assembly via adaptive κ-mer weighting
642 and repeat separation. *Genome Res.* Advance Access published 2017,
643 doi:10.1101/gr.215087.116.
644 **Krohn-Molt, I., Alawi, M., Förstner, K. U., Wiegandt, A., Burkhardt, L., Indenbirken,**
645 **D., Thieß, M., Grundhoff, A., Kehr, J., Tholey, A., et al.** (2017). Insights into
646 Microalga and bacteria interactions of selected phycosphere biofilms using

647 metagenomic, transcriptomic, and proteomic approaches. *Front. Microbiol.* **8**.
648 **Kumar, S., Stecher, G., and Tamura, K.** (2016). MEGA7: Molecular Evolutionary Genetics
649 Analysis Version 7.0 for Bigger Datasets. *Mol. Biol. Evol.* **33**:1870–1874.
650 **Langmead, B., and Salzberg, S. L.** (2012). Fast gapped-read alignment with Bowtie 2. *Nat.*
651 *Methods* **9**:357–359.
652 **Ley, R. E., Hamady, M., Lozupone, C., Turnbaugh, P. J., Ramey, R. R., Bircher, J. S.,**
653 **Schlegel, M. L., Tucker, T. A., Schrenzel, M. D., Knight, R., et al.** (2008). Evolution
654 of Mammals and Their Gut Microbes. *Science (80-.).* **320**:1647 LP – 1651.
655 **Li, H., and Wren, J.** (2014). Toward better understanding of artifacts in variant calling from
656 high-coverage samples. *Bioinformatics* Advance Access published 2014,
657 doi:10.1093/bioinformatics/btu356.
658 **Li, H., Handsaker, B., Wysoker, A., Fennell, T., Ruan, J., Homer, N., Marth, G.,**
659 **Abecasis, G., and Durbin, R.** (2009). The Sequence Alignment/Map format and
660 SAMtools. *Bioinformatics* **25**:2078–2079.
661 **Liebe, S., Wibberg, D., Winkler, A., Puehler, A., Schlueter, A., and Varrelmann, M.**
662 (2016). Taxonomic analysis of the microbial community in stored sugar beets using
663 high-throughput sequencing of different marker genes. *FEMS Microbiol. Ecol.* **92**:1–12.
664 **Magoč, T., and Salzberg, S. L.** (2011). FLASH: Fast length adjustment of short reads to
665 improve genome assemblies. *Bioinformatics* **27**:2957–2963.
666 **Marschner, P.** (2011). *Marschner's Mineral Nutrition of Higher Plants: Third Edition*.
667 **Maus, I., Kim, Y. S., Wibberg, D., Stolze, Y., Off, S., Antonczyk, S., Pühler, A., Scherer,**
668 **P., and Schlüter, A.** (2017). Biphasic Study to Characterize Agricultural Biogas Plants
669 by High-Throughput 16S rRNA Gene Amplicon Sequencing and Microscopic Analysis.
670 *J. Microbiol. Biotechnol.* **27**.
671 **McKirdy, D. M., Cox, R. E., Volkman, J. K., and Howell, V. J.** (1986). Botryococcane in a
672 new class of Australian non-marine crude oils. *Nature* **320**:57–59.
673 **Meyer, F., Goesmann, A., McHardy, A. C., Bartels, D., Bekel, T., Clausen, J.,**
674 **Kalinowski, J., Linke, B., Rupp, O., Giegerich, R., et al.** (2003). GenDB - An open
675 source genome annotation system for prokaryote genomes. *Nucleic Acids Res.* **31**:2187–
676 2195.
677 **Molnár, I., Lopez, D., Wisecaver, J. H., Devarenne, T. P., Weiss, T. L., Pellegrini, M.,**
678 **and Hackett, J. D.** (2012). Bio-crude transcriptomics: gene discovery and metabolic
679 network reconstruction for the biosynthesis of the terpenome of the hydrocarbon oil-
680 producing green alga, Botryococcus braunii race B (Showa). *BMC Genomics* **13**:576.

Nguyen, C. (2003). Rhizodeposition of organic C by plants: mechanisms and controls Advance Access published 2003.

O'Leary, N. A., Wright, M. W., Brister, J. R., Ciufo, S., Haddad, D., McVeigh, R., Rajput, B., Robbertse, B., Smith-White, B., Ako-Adjei, D., et al. (2016). Reference sequence (RefSeq) database at NCBI: Current status, taxonomic expansion, and functional annotation. *Nucleic Acids Res.* **44**:D733–D745.

Pančić, M., and Kiørboe, T. (2018). Phytoplankton defence mechanisms: traits and trade-offs. *Biol. Rev.* **93**:1269–1303.

Price, M. N., Dehal, P. S., and Arkin, A. P. (2010). FastTree 2 - Approximately maximum-likelihood trees for large alignments. *PLoS One* **5**.

Ramanan, R., Kim, B.-H., Cho, D.-H., Oh, H.-M., and Kim, H.-S. (2016). Algae–bacteria interactions: Evolution, ecology and emerging applications. *Biotechnol. Adv.* **34**:14–29.

Reed, H., and Martiny, J. (2007). Testing the functional significance of microbial composition in natural communities. *FEMS Microbiol. Ecol.* **62**:161–170.

Rivett, D. W., and Bell, T. (2018). Abundance determines the functional role of bacterial phylotypes in complex communities. *Nat. Microbiol.* **3**:767–772.

Rojo, F. (2010). Enzymes for Aerobic Degradation of Alkanes. In *Handbook of Hydrocarbon and Lipid Microbiology* (ed. Timmis, K. N.), pp. 781–797. Berlin, Heidelberg: Springer Berlin Heidelberg.

Sambles, C., Moore, K., Lux, T. M., Jones, K., Littlejohn, G. R., Gouveia, J. D., Aves, S. J., Studholme, D. J., Lee, R., and Love, J. (2017). Metagenomic analysis of the complex microbial consortium associated with cultures of the oil-rich alga Botryococcus braunii. *Microbiologyopen* **6**.

Sañudo-Wilhelmy, S. A., Gómez-Consarnau, L., Suffridge, C., and Webb, E. A. (2014). The Role of B Vitamins in Marine Biogeochemistry. *Ann. Rev. Mar. Sci.* **6**:339–367.

Schlegel, H. G., Kaltwasser, H., and Gottschalk, G. (1961). Ein Submersverfahren zur Kultur wasserstoffoxydierender Bakterien: Wachstumsphysiologische Untersuchungen. *Arch. Mikrobiol.* **38**:209–222.

Schreiter, S., Ding, G.-C., Heuer, H., Neumann, G., Sandmann, M., Grosch, R., Kropf, S., and Smalla, K. (2014). Effect of the soil type on the microbiome in the rhizosphere of field-grown lettuce. *Front. Microbiol.* **5**:144.

Schwarzhans, J. P., Cholewa, D., Grimm, P., Beshay, U., Risse, J. M., Friehs, K., and Flaschel, E. (2014). Dependency of the fatty acid composition of Euglena gracilis on growth phase and culture conditions. *J. Appl. Phycol.* **27**:1389–1399.

715 **Seemann, T.** (2014). Prokka: Rapid prokaryotic genome annotation. *Bioinformatics* **30**:2068–
716 2069.
717 **Seymour, J. R., Amin, S. A., Raina, J. B., and Stocker, R.** (2017). Zooming in on the
718 phycosphere: The ecological interface for phytoplankton-bacteria relationships. *Nat.*
719 *Microbiol.* **2**.
720 **Simão, F. A., Waterhouse, R. M., Ioannidis, P., Kriventseva, E. V., and Zdobnov, E. M.**
721 (2015). BUSCO: Assessing genome assembly and annotation completeness with single-
722 copy orthologs. *Bioinformatics* **31**:3210–3212.
723 **Takahashi, S., Tomita, J., Nishioka, K., Hisada, T., and Nishijima, M.** (2014).
724 Development of a prokaryotic universal primer for simultaneous analysis of bacteria and
725 archaea using next-generation sequencing. *PLoS One* **9**:e105592.
726 **Tanabe, Y., Okazaki, Y., Yoshida, M., Matsuura, H., Kai, A., Shiratori, T., Ishida, K. I.,**
727 **Nakano, S. I., and Watanabe, M. M.** (2015). A novel alphaproteobacterial
728 ectosymbiont promotes the growth of the hydrocarbon-rich green alga Botryococcus
729 braunii. *Sci. Rep.* **5**.
730 **Tang, Y. Z., Koch, F., and Gobler, C. J.** (2010). Most harmful algal bloom species are
731 vitamin B1 and B12 auxotrophs. *Proc. Natl. Acad. Sci.* **107**:20756–20761.
732 **Walker, B. J., Abeel, T., Shea, T., Priest, M., Abouelliel, A., Sakthikumar, S., Cuomo, C.**
733 **A., Zeng, Q., Wortman, J., Young, S. K., et al.** (2014). Pilon: An integrated tool for
734 comprehensive microbial variant detection and genome assembly improvement. *PLoS*
735 *One* Advance Access published 2014, doi:10.1371/journal.pone.0112963.
736 **Wang, Q., Garrity, G. M., Tiedje, J. M., and Cole, J. R.** (2007). Naive Bayesian classifier
737 for rapid assignment of rRNA sequences into the new bacterial taxonomy. *Appl. Environ.*
738 *Microbiol.* **73**:5261–5267.
739 **Wang, X., Li, Z., Su, J., Tian, Y., Ning, X., Hong, H., and Zheng, T.** (2010). Lysis of a
740 red-tide causing alga, Alexandrium tamarense, caused by bacteria from its phycosphere.
741 *Biol. Control* **52**:123–130.
742 **Waterhouse, R. M., Seppey, M., Simao, F. A., Manni, M., Ioannidis, P., Klioutchnikov,**
743 **G., Kriventseva, E. V., and Zdobnov, E. M.** (2018). BUSCO applications from quality
744 assessments to gene prediction and phylogenomics. *Mol. Biol. Evol.* **35**:543–548.
745 **Wibberg, D., Blom, J., Jaenicke, S., Kollin, F., Rupp, O., Scharf, B., Schneiker-Bekel, S.,**
746 **Sczcepanowski, R., Goesmann, A., Setubal, J. C., et al.** (2011). Complete genome
747 sequencing of Agrobacterium sp. H13-3, the former Rhizobium lupini H13-3, reveals a
748 tripartite genome consisting of a circular and a linear chromosome and an accessory

749 plasmid but lacking a tumor-inducing Ti-plasmid. *J. Biotechnol.* **155**:50–62.
750 **Wibberg, D., Andersson, L., Rupp, O., Goesmann, A., Pühler, A., Varrelmann, M.,**
751 **Dixelius, C., and Schlüter, A.** (2016). Genome analysis of the sugar beet pathogen
752 Rhizoctonia solani AG2-2IIIB revealed high numbers in secreted proteins and cell wall
753 degrading enzymes. *BMC Genomics* Advance Access published 2016,
754 doi:10.1186/s12864-016-2561-1.
755 **Xu, J., Zhang, Y., Zhang, P., Trivedi, P., Riera, N., Wang, Y., Liu, X., Fan, G., Tang, J.,**
756 **Coletta-Filho, H. D., et al.** (2018). The structure and function of the global citrus
757 rhizosphere microbiome. *Nat. Commun.* **9**:4894.
758 **Zengler, K., and Zaramela, L. S.** (2018). The social network of microorganisms - How
759 auxotrophies shape complex communities. *Nat. Rev. Microbiol.* Advance Access
760 published 2018, doi:10.1038/s41579-018-0004-5.
761 **Zhang, H., Yohe, T., Huang, L., Entwistle, S., Wu, P., Yang, Z., Busk, P. K., Xu, Y., and**
762 **Yin, Y.** (2018). dbCAN2: a meta server for automated carbohydrate-active enzyme
763 annotation. *Nucleic Acids Res.* Advance Access published 2018,
764 doi:10.1093/nar/gky418.
765 **Zhou, J., Bruns, M. A., and Tiedje, J. M.** (1996). DNA recovery from soils of diverse
766 composition. *Appl. Environ. Microbiol.* **62**:316–322.
767
768
769 **Additional files**

770 **Supplementary Materials.**
771 Figure S1: Characteristics and taxonomic profiling of xenic *Botryococcus braunii* race A and
772 B cultures. Illustrated are the typical colony-forming cells of *B. braunii* races A and B with a
773 complex structure size of approximately >100µm in diameter. The table shows the mean
774 values (three biological and technical replicates, SE; n=9) of algal content of biomass,
775 hydrocarbons and carbohydrates at the sampling time points (linear and stationary growth
776 phases). DW, culture dry weight.

777 Figure S2: Taxonomic profiling of *Botryococcus braunii* associating community. Relative
778 abundance of detected taxa (phylum level) based on (**a**) high-throughput 16S rRNA gene
779 amplicons and (**b**) metagenomic reads. The evaluation of 16S rDNA amplicons are detailed in
780 Table S3. Metagenome datasets were taxonomically assigned via MEGAN (200,000
781 randomly subsampled reads, minimum 50 reads per taxonomic group). The relatively high

782 proportion of unassigned reads likely results from the fact that the algal and some bacterial
783 genomes are not disposed in the used NCBI-NR database. The analysis revealed the
784 occurrence of the phyla Euryarchaeota and Viruses belonging to the family of *Microviridae*
785 (bacteriophages with a single-stranded DNA genome).

786 Figure S3: Microbiome accompanying the *Botryococcus braunii* consortia. Illustration of the
787 relative abundance and phylogenetic distribution of bacterial genera detected via high-
788 throughput 16S rDNA amplicon sequencing approach (for details see Table S3).

789 Figure S4: Phylogenetic classification of selected *Botryococcus braunii* consortia members.
790 Illustrated is the phylogenetic characterization of the high-quality draft and complete genomes
791 of *B. braunii* accompanying bacterial community. Maximum-likelihood-based phylogenetic
792 tree built out of a core of 53 conserved marker genes (Table S4) per analyzed genome (bold).
793 Black, grey and white circles represent the nodes with calculated bootstrap values of 100, 99
794 and <75%, respectively (1,000 replicates).

795 Figure S5: Comparison and taxonomic assignment of different *Botryococcus braunii*
796 metagenomes. Datasets obtained during the present study (races A and B, T1 and T2 (linear
797 and stationary growth phases, respectively) were compared to the datasets of Guadeloupe race
798 B strain (Condition A-C supplemented with citric acid as organic carbon source and vitamins
799 (B_1, B_7 and B_{12}), with A: initial consortium, B: washed culture, C: antibiotics-treated
800 (ciprofloxacin)) (Sambles et al. 2017). For each sample, 200,000 metagenomic reads were
801 randomly subsampled and subjected to the taxonomic assignment using DIAMOND and
802 MEGAN (minimum 50 reads per taxonomic group). The circle size represents the amount of
803 classified reads for the respective taxonomic group.

804 Figure S6: Hydrocarbon accumulation profiles of axenic and xenic *B. braunii* cultures. Shown
805 is the hydrocarbon content observed in the samples of (**a**) axenic *B. braunii* (green) as well as
806 in presence of (**b**) *Mycobacterium* sp. Bb-A (orange) and (**c**) *Brevundimonas* sp. Bb-A (blue)
807 during the course of cultivation. The data serves as additional information for Figure 2.

808 Table S1: Features of the metagenome assembled genomes (MAGs). Assembly and
809 annotation characteristics (*e.g.* Total size, N50, etc.) are listed according to the respective
810 MAG. The completeness as well as the contamination degree of the MAGs was assessed via
811 BUSCO (v3.0.). P- and E-Modi refer to prokaryotic MAGs and eukaryotic genome fragments,
812 respectively. The high-quality MAGs were classified via single-copy marker genes, *e.g. rpoB*,

813 *rpoD* etc., detected by BUSCO. The metagenomic datasets of *B. braunii* race A and B were
814 mapped against the MAGs, and represented as percentage of mapped reads.

815 Table S2: Characteristics of high-quality draft and complete genomes. Summary of the
816 taxonomy distribution and annotation features of ten high-quality MAGs and two complete
817 genomes (completeness >80%, contamination <10%, Table S2) obtained from the *B. braunii*
818 race A and B consortia. Shown are similarity mean values based on AAI (genome to genome
819 comparison). Genomes with similarity values >95% are regarded as the same species as the
820 reference. MAG, metagenome assembled genome; AAI, average amino acid identities; CDS,
821 Coding DNA sequences.

822 Supplementary Discussion
823 Chapter 1 | Metagenomic survey of the *Botryococcus braunii* consortia
824 Chapter 2 | Elucidation of the genetic portfolio of the bacterial community
825

826 **Supplementary Tables.** (XLSX**,** 330 KB)

827 Table S3: Statistics and taxonomic classification of 16S rRNA gene amplicon sequencing of
828 the *B. braunii* consortia. Datasets include the analysis of the high-throughput 16S rDNA
829 amplicon sequencing results and are supplemental information for Figures S2a and S3.
830 Abbreviations: OTU, operational taxonomic unit; T, time point.

831 Table S4: List of conserved core genes. Dataset serves as supplemental information for Figure
832 S4 and includes conserved marker (core) genes shared among the 31 genomes, used for the
833 construction of the Maximum-likelihood-based (ML) phylogenetic tree.

834 Table S5: List of all detected functional pathways encoded in the high-quality draft and
835 complete bacterial genomes. Datasets include KEGG-based functionally assigned pathways of
836 the annotated high-quality MAGs and complete genomes imported to the EMGB platform.
837 (elastic metagenome browser, https://emgb.cebitec.uni-bielefeld.de/Bbraunii-bacterial-
838 consortium/). Displayed are the total number of the enzymes and the corresponding EC
839 numbers encoded within the particular genome for the respective pathway. Bold marked
840 pathway maps have been selected for Figure 1b.

841 Table S6: List of selected manually inspected genes within the high-quality draft and
842 complete bacterial genomes. Datasets include manual BLASTp screening results (E-value
843 threshold $1x10^{-10}$) of selected genes.

844 Table S7: List of Carbohydrate-active enzymes (CAZy) encoded by the *B. braunii* bacterial
845 community members. Datasets include Carbohydrate-active enzymes (CAZy) encoded within
846 the high-quality draft and complete bacterial genomes and serve as additional information for
847 Figure 1b. The gene search within the high-quality draft and complete genomes was
848 accomplished via dbCAN2 metaserver (Zhang et al. 2018).

849 Table S8: List of all detected B-vitamin biosynthesis genes encoded by the *B. braunii*
850 bacterial community members. Datasets include the function description (EC number) as well
851 as the corresponding genes of the key enzymes involved in the de novo biosynthesis of B-
852 vitamins and serve as supplemental information for Figure 3a. The genes involved in the
853 particular B-Vitamin pathway were searched (based on EMGB annotation system and manual
854 BLASTp search) within the high-quality draft and complete bacterial genomes. √*, alternative
855 gene identified via manual BLASTp search. Abbreviations: *M*. Bb-A, *Mycobacterium* sp. Bb-
856 A; *B*. Bb-A, *Brevundimonas* sp. Bb-A; *P*.Bb-B, *Pimelobacter* sp. Bb-B.

857 Table S9: List of all detected secondary metabolite biosynthetic gene clusters. The datasets
858 include the identified secondary metabolite biosynthetic gene clusters encoded by the high-
859 quality draft and complete genomes of the *B. braunii* associates and serve as additional
860 information for Figure 1b. The analysis was accomplished using the antibiotics & Secondary
861 Metabolite Analysis Shell (antiSMASH, Version 4.1.0, Blin et al. 2017).
862